Intra-deltaic Faulting: Determining How Strain is Distributed Across a Salt Minibasin, Northern Gulf of Mexico

University of Houston
Department of Geosciences
MS Thesis Proposal

Leigh Owens

Advisor: Dr. Bhattacharya, UH
Committee Members:
Dr. Murphy, UH
Dr. Liner, UH
Dr. Gillian Apps, BP, Houston

Abstract

3D seismic data allows for the evaluation of synsedimentary intra-deltaic deformation within a Plio-Pleistocene shelf margin delta in a salt dome minibasin in the northern Gulf of Mexico. This area is dominated by salt tectonics and the continental shelf and shelf edge lies in two tectono-stratigraphic provinces: the Plio-Pleistocene detachment province and the salt dome minibasin province. These minibasins are flanked by salt diapirs and infilled with Paleo-Mississippi deltaic deposits.

This study focuses on one growth faulted shelf edge delta in a minibasin in the Green Canyon block. The goal of the study is to determine the interplay between growth faulting and sedimentation and how strain is distributed throughout this minibasin. Preliminary interpretation of a few 2D seismic lines suggest growth faults within a deltaic system sole into a common horizon and lie stratigraphically within prograding delta lobes. However, it is uncertain whether this relationship is basinwide. This investigation tests two hypotheses which explain the relationship between growth faulting and sedimentation. Hypothesis 1 predicts growth faulting in response to a point-sourced, localized sedimentary body (bars and lobes). Hypothesis 2 predicts growth faulting in response to distributed strain, indicated by a composite fault array that cross-cuts lobes and faults in response to a gravitational slumping of the broader continental margin.

High-resolution 3D seismic amplitude and coherency data will allow for the imaging of seismic sedimentological and geomorphological features and deltaic growth successions of adjacent fault blocks within the delta. The structural analysis will include the evaluation of fault geometries, fault linkage, and fault timing using 3D seismic data to determine if growth faulting is in response to localized or distributed strain. This study is significant because the formation of growth faults represents the critical sediment balance between loads in passive margins or deltas.

Introduction

Deltaic growth faults and associated strata record the interaction between sedimentary processes and fault movements. Deltas are the means by which shelves and shelf margins grow in a basinward direction. The internal geometries of deltas are significant in controlling sediment pathways across the shelf and onto the slope and basinal settings, as well as forming an important class of reservoir. Deltaic systems are commonly complicated by growth faults due to the formation of thicker, sand-dominated successions accumulating on the downthrown side towards the basin and the formation of traps created in hanging-wall rollover anticlines. Growth faults are important reservoirs for oil and gas, as they form thick, wedge-shaped sand packages that may be up to 100's of meters thick and laterally continuous on the order of 10's to 100's of kilometers (Galloway *et al.,* 1982).

2D seismic studies of shelf margin deltas in the Gulf of Mexico show growth faults (Roberts and Sydow, 2003; Anderson *et al.,* 2004; Wellner *et al*., 2004; Robert *et al.,* 2004; Abdulah *et al.,* 2004) but lack 3D representation of deformation features and the distribution of lithologies.

Deltaic growth faults are hypothesized to form in two ways; differential compaction of shale layers in a sandstone-shale sequence, and by gravity sliding toward the basin. In the Gulf of Mexico, both mechanisms are operative. This study will evaluate which mechanism is more important in the formation of growth faults. Two hypotheses will be tested; growth faulting in response to localized strain, in

which point sourced loads, like bars or lobes, causes the faulting or distributive strain, which is due to regional extension on the continental margin.

The focus of this project is to determine how strain is distributed across the minibasin and how growth faulting links to the deltaic processes of an unstable continental margin. The two end members of growth faulting mechanisms, local and distributive strain, can be imaged in plan view by analyzing their structural geology to see how the faults are linked and how strain is distributed. This study is an opportunity to test ideas on how inter-deltaic growth faults form. This 3D seismic dataset will allow for the evaluation of the size and scale of the architectural elements that drive the strain and appearance of the growth faults. Utilizing plan view and cross-sectional analysis and structural geology methods will lead to the determination of point- versus regional-sourced strain and how this may be reflected in different faulting patterns and linkages.

As well as imaging 3D fault linkages and fault arrays, structural geology methods will be used to analyze these growth faults. Throw versus depth plots have been used in both 2D and 3D seismic datasets for the kinematic analyses of growth faults (Tearpock and Bischke, 1991; Bischke, 1994; Cartwright *et al.,* 1998; Castelltort *et al*., 2004; Back *et al*., 2006). Back *et al*., (2006), utilized 3D seismic coherency data and throw versus depth plots to establish stratigraphic correlations between deltaic growth successions of adjacent fault blocks in the Niger Delta. In this study, a similar interpretation workflow will be utilized to determine the interplay between growth faulting and sedimentation.

Growth faulted deltas

Point-sourced growth faults

Many small-scale growth faulted deltas have been studied in outcrop. Early outcrop studies of these growth faults (Brown *et al*., 1973; Edwards, 1976; Rider, 1978) concluded that growth faults occur in areas of high sedimentation rates, where dense sand packages overlie mobile muds such as in the prodelta to delta front transition. Edwards (1976) describes growth faulting on the scale of 150 m in Upper Triassic Deltaic systems, in coastal cliffs in southeast Svalbard in which the development of the delta depends on the balance between the rate of sedimentation and the rate of subsidence. Edwards suggests the initiation of faulting may be due to 1) denser sands overlying less dense clays, 2) southward progradation of prodelta slope, 3) differential loading associated with deltaic progradation, 4) triggering mechanism such as earthquakes. Edwards (1976) determined that the upper tips of the listric growth faults terminate at the muddy facies of the overlying flooded surface, while the lower segments of the faults sole into the prodelta muds that lie under the prograding sand.

Evamy *et al*., (1978) describe growth faulting of the Niger Delta on scales of 2000 to 3000m. They show growth faults initiate when heavy, sandy deposits of a regressive cycle (Rd> Rs) prograde over clays with low shear strength. Figure 1 (modified after Bruce, 1973) shows a schematic of the development of growth faults under conditions of a prograding delta. The amount of space created by individual growth faults is insufficient to accommodate the supply of sediment. New, fault-

controlled depocenters are formed progressively in a seaward direction. If there is no change in Rd/Rs ratio, then all successive depocenters are part of the same sedimentary unit. They also show that counter-regional faults from where Rd=Rs.

Bhattacharya and Davies (2001, 2004) describe growth faulting within one delta (10 meter scale), the Ferron Last Chance Delta in Muddy Creek, Utah prograding over a shallow intracratonic seaways. They were able to kinematically restore the sequence of the faults (Fig. 2), by identifying pregrowth, growth, and post growth strata. They determined that the initiation of growth faults is not systematic and moves basinward or landward as depositional loci switch. A similar scale study by Wignall and Best (2004), describes growth faulting on a scale of 60 m initiated from a point-sourced loading in which the fault complex records a landward retrogressive movement, with only one fault active at one time.

Regional growth faults

The point-sourced growth faults contrast with growth faults that form by slope failure prior to deposition of the next delta on the shelf edge. Diegal *et al*., (1995) describes the large arcuate growth faults systems in the Gulf of Mexico (Fig.3). Many subsurface studies of growth faults involve continental shelf margins, where deltas prograde to the shelf edge causing gravitational forces to initiate slumps and faults (Brown *et al.*, 2004; Owoyemi and Willis, 2006). These faults are regional scale, single event, slope collapse features that record the extensional development of growth faults and are easily observed in high quality seismic data.

Nemec *et al.,* (1988) cites gravitational instability on delta front slopes of Eastern Spitsbergen that causes growth faulting within a unit that is 50 m thick.

Brown *et al*., (2004) concludes that delta deposition during lowstand of sea level exerted sufficient gravity stress to trigger large sections of the outer shelf and slope strata to fail and shift basinward (Fig. 4). This continental margin gravity slumping cross-cuts multiple deltaic parasequences during regional extension. But Brown *et al.,* (2004) shows no relay ramps.

Owoyemi and Willis (2006) show large-scale growth faults on the order of 2km formed by continental-margin collapse (Fig. 5) that shows the thinning of successive sequences upward, basinward shift of deposition, and decrease in the vertical offset of reflections across faults, suggesting that the rate of fault movement decreased over time.

Different structural styles of growth faults relate to the position on the shelf versus the basin and different stress mechanisms. The point-sourced Ferron sandstone (Bhattacharya and Davies, 2001, 2004) is analogous to the inner-shelf. The regional-scale growth faults that initiate due to gravity-driven slumping are typical at the continental margin.

Geologic Setting

Tectonic evolution of the Texas-Louisiana continental shelf is largely controlled by salt deposition and withdrawal forming an extensional regime. Accommodation in the Gulf of Mexico is created by changes in eustatic sea level, salt

withdrawal, large scale growth faulting, and local and regional subsidence (Winker and Edwards, 1983). Diegel *et al.,* (1995), divides the Northern Gulf of Mexico into multiple tectono-stratigraphic provinces (Fig. 3). The study area lies in the salt-dome minibasin province to the north and the Plio-Pleistocene detatchement province to the south.

The Gulf of Mexico Basin formed as a result of the southward drift of the Yucatan continental block away from the North American Plate. Rifting, accompanied by salt deposition in the Jurassic, created the Gulf basin (Salvador, 1987; Diegal *et al.,* 1995). The Louann Salt was deposited during the Upper Jurassic (Peel et al., 1995). During the Cenozoic, thick salt deposits were remobilized by large sediment loads delivered to the shelf by river-delta systems. Salt diapirism (Fig. 6) created additional accommodation in the form of minibasins that were able to collect and contain sediment from later prograding deltas (Ge *et al*., 1997). The Paleo-Mississippi river system supplied sediments to the northern Gulf of Mexico during the Pleistocene (Galloway *et al*., 2000).

Study Area

The study area (Fig. 3) is located in the northern Gulf of Mexico, about 150 km south of Louisiana, and covers the shelf margin and upper slope. The water depths are between 185 and 375 meters. This research is focused on one minibasin in the Green Canyon block that is flanked by residual vertical salt bodies to the northwest and the southeast (Fig. 7, 8a). This Cenozoic-aged minibasin is 384

square kilometers in area and is 16 km long and 24 km wide. It is bound by inlines 27970 to 29370 and crosslines 7118 to 5198.

The interval of interest within this minibasin is one deltaic sequence that is internally deformed. This intra-deltaic deformation is indicated by a series of growth faults, fully contained within the delta. The growth faulting in this interval is in a single sequence of deltaic progradation (Fig. 8b). In this interval, discontinuous, landward dipping reflections are contained within a series of listric, normal faults that dip basinward.

Despite being contained in an area of active salt tectonics, growth strata are largely confined within the delta complex, in contrast to regional growth faults that offset numerous stacked complexes in the Gulf of Mexico (Brown *et al*., 2004) and other systems like the Niger delta (Evamy *et al.,* 1978; Owoyemi and Willis, 2006; Back *et al*., 2006).

Kinematic analysis of growth faults

This study is significant because the formation of growth faults represents a critical sediment balance between loads in passive margins or deltas. Sedimentation rates of the shelf and upper slope environments are commonly nearly equal to fault displacement rates (Cartwright *et al*., 1998; Castelltort *et al*., 2004; Back *et al*., 2006). Thickness changes across growth faults allow the amount of throw that accumulated during deposition to be calculated (Thorsen, 1963; Edwards, 1995; Baudon and Cartwright, 2008).

Growth faults record the interactions between slip history and sedimentation and can be studied by kinematic analysis conceptually established by Wadsworth (1953) and Thorsen (1963). The expansion index , E.I., (Fig. 9) is a widely used measure of growth faulting and is important in defining periods of significant growth (Thorsen, 1963; McCulloh, 1988; Edwards, 1995), however because it is a ratio it does not give information on slip rate (Cartwright *et al*., 1998).

Instead, a throw versus depth plot 'T-Z plot' (Fig. 10) is used as the main tool for kinematic analysis because it contains information of absolute slip for time intervals defined by correlative stratigraphic units across faults (Mansfield and Cartwright, 1996; Cartwright *et al.,* 1998). A throw versus depth plot is a simple geometric tool that graphically represents stratal thickness variations in a growth fault setting by plotting the throw of sedimentary horizons versus their depth in the hanging wall and has been used to infer fault kinematics (Tearpock and Bischke, 1991; Bischke, 1994; Castelltort *et al.,* 2004; Cartwright *et al*., 1998). Cartwright *et al*., (1998) utilized these graphical techniques to analyze the kinematic evolution of 17 growth faults from offshore Texas. They constructed T-Z plots for each fault and also analyzed the kinematic behavior of all the faults in the transect for any systematic activity by defining the growth and nongrowth intervals and correlated these using seismic horizons (Fig. 11). The T-Z plot can also provide information about the fault topography from in-filling sedimentation, which can be used as a predication tool for lithologic change using only seismic data (Castelltort *et al*., 2004; Pochat *et al*., 2004; Back *et al*., 2006).

These two common methods for growth fault systems (expansion index measurement and throw versus depth plots) were originally developed for the analysis of 2D data and Back *et al*., (2006), used a high-resolution 3D seismic database from the Niger Delta to provide 3D information on the development of faults, unit thicknesses, and depositional systems over time. The Niger Delta database consists of four fault blocks bounded by kilometer-scale, basinward-dipping, synsedimentary faults, and they use 3D seismic coherency data (Fig. 12) on horizon-slices to support the correlation of growth successions from one fault block to another. They state the seismic interpretation workflow in the Niger Delta case study by Back *et al*., (2006) can be applied directly to establish repeatable correlations of growth strata in a variety of settings that are characterized by syntectonic sedimentation. Additionally, they apply the throw versus depth method analysis to the 3D seismic data.

Baudon and Cartwright (2008) analyzed the geometry and kinematic evolution of small growth faults from a high-resolution 3D seismic dataset from the Levant Basin, in the eastern Mediterranean. They were able to evaluate the 3D geometry, distribution of throw, and the segmentation history of one fault. Horizons were mapped for 14 stratigraphic levels and throw measurements were displayed on a T-Z plot as individual plots of a single transect. They also created a structural map, dip map, and fault gap map, as well as a visualization of the fault geometry (Fig. 13). The dip map was used to depict the fault trace and create a schematic of the lateral segment linkage of faults (Fig. 14). Baudon and Cartwright (2008) were also able to map river channels and find that they were diverted in the synkinematic

package and continuous in the prekinematic package, based on their throw interpretation (Fig.15).

Methods

Data

The 3D seismic data used for this study is a portion of an 8000 square kilometer prestack migrated seismic survey that was acquired by Petroleum Geo-Sciences (PGS) and donated to the University of Houston. This study uses 384 square km of the Green Canyon block. The survey is enclosed between latitudes 27° 50' N – 28° 10'N and 92°11'W - 92° 23'W. Horizontal resolution is defined by the distance between the in-lines, 25 m, and cross lines, 37.5m. The 3D seismic dataset is one-second, two-way travel time. To convert two-way-travel times to depth units, the linear v(z) equation, $v(z)= v_0+ kz$ was used, where v_0 is 1500 m/s, k is the velocity gradient of 0.4, and z is the depth in meters (Liner, 2004) and for thickness calculations of units. The thickness of the interval of interest (Fig. 8b) is calculated to be 560 m and the water depth ranges from 190 m to 415 m. Well logs are available for this study area, so chronostratigraphic data may be acquired.

Structural Analysis

In order to test how inter-deltaic growth faults form, two faulting mechanisms will be evaluated; point-sourced stress and distributive stress. Hypothesis 1 (Fig. 16) depicts growth faulting in response to a point-sourced, localized sedimentary body (bars and lobes). The prediction is point- sourced faults

form within the delta lobe. Hypothesis 2 (Fig. 17) depicts growth faulting in response to distributed strain indicated by a composite fault array that cross-cuts lobes and forms in response to a regional extension of the continental margin.

Hypothesis 1 predicts faults in plan view are contained only within the delta lobe. For hypothesis 1, the prediction is that faults would be confined within one deltaic sequence and sole into a common horizon or detachment that would correspond to a shale body. The predicted depth of the fault, would be equal to or less than the depth of the sedimentary body. Hypothesis 1 predicts smaller fault lengths, more isolated faults and less fault linkage, less branching and compression features at fault tips that would show the early stages of linking may be present.

Hypothesis 2 predicts growth fault system to exceed the size of depositional features. Hypothesis 2 predicts the faults would not be confined within one sequence or facies pair, but continue regionally and would crosscut multiple sequences. The faults are not predicted to sole into a common horizon or detachment and would not correspond to a specific sedimentary feature. The predicted depth of the fault would be greater than or equal to depth of the sedimentary body. Compression features in plan view are not predicted in hypothesis 2, however relay ramps and larger faults in length and displacement due to linking and branching are expected.

In order to test these two hypotheses, a series of questions will be evaluated for each hypothesis;

1) Are the faults planar versus listric?

2) Do the faults sole into a common horizon or detachment surface? and if so, does it correspond to a particular sedimentary layer?

3) How did the fault system nucleate or evolve? Did it form from multiple faults, linking, and if so, how many?

4) What is the sequence of growth faulting within the fault system?

Data reconnaissance through successive vertical, horizon slices and diagonal intersections will be done using Petrel, seismic interpretation software. Seismic will be flattened along horizons to remove the effects of salt diapiric deformation and to determine the seismic geomorphology of the layers. Structural analysis will include the evaluation of fault geometries, fault linkage, and fault timing using 3D seismic data.

The faults will be mapped and picked along individual fault blocks within a 2D seismic window, which includes across fault correlation based on visual similarity of reflections. Faults will be imaged using seismic attributes such as coherency, ant tracking, and max-min curvature. Fault mapping will determine the fault geometries, planar or listric, and the spatial extent (along strike) distance and if the faults sole into a common horizon or detachment surface.

A time-depth conversion will be performed on the data. The hangingwall and footwall cutoffs will be mapped to determine throw of the faults and create a fault gap map. Fault linkage will be determined by creating displacement versus length

plots to evaluate how the fault system nucleated or evolved. This plot will show if the fault system formed from multiple faults by linking and if so, how many.

Fault timing will be attempted based on expansion features in the growth fault system by mapping unique reflection patterns across fault blocks. A preliminary 2D interpretation depicts the mapping of growth faults, continuous reflections within the rotated blocks, and infilling sediment on both a non-flattened horizon (Fig. 18a) and a flattened horizon (Fig. 18b). Also, a throw versus depth plot will show the periods of active versus inactivity along the fault.

Finally, a detailed analysis of the coherence horizon slices will be done to find stratigraphic patterns that correlate across faults. Ideally this will result in finding depositional elements (e.g. channels) that link the footwall and hanging wall of fault blocks. The faults will be analyzed in plan view of in the scale of the minibasin and then will be searched for on a broader scale to image potential regional-scale growth faults across the entire dataset that contains multiple minibasins.

Conclusion

Preliminary interpretation of growth faults within a Gulf of Mexico shelf edge deltaic system show that faults sole into a common horizon and lie stratigraphically beneath prograding delta lobes. However, it is uncertain whether this relationship is local or regional. This investigation uses 3D seismic data and tests two hypotheses to determine how strain is distributed across the minibasin and how growth faulting links to the deltaic processes of an unstable continental margin. Hypothesis 1 predicts growth faulting in response to a point-sourced, localized sedimentary

body. Hypothesis 2 predicts growth faulting in response to distributed strain, indicated by a composite fault array that cross-cuts lobes and faults in response to a gravitational slumping of the continental margin. This study is significant because the formation of growth faults represents the critical sediment balance between loads in passive margins or deltas.

Bibliography

Alexander, L.L., and Flemings, P.B., 1995, Geologic evolution of a Pliocene-Pleistocene salt-withdrawal minibasin: Eugene Island Block 330, Offshore Louisiana: AAPG Bulletin, v. 79, no. 12, p. 1737-1756.

Anderson, J.E., Cartwright, J., Drysdall, S.J., Vivian, N., 2000, Controls on turbidite sand deposition during gravity-driven extension of a passive margin: Examples from Miocene sediments in Block 4, Angola: Marine and Petroleum Geology, v. 17, p. 1165-1203.

Anderson, J.B., Rodriguez, A., Abdulah, K.C., Fillon, R.H., Banfield, L.A., McKeown, H.A., and Wellner, J.S., 2004, Late Quaternary stratigraphic evolution of the Northern Gulf of Mexico margin: A synthesis, *in* Anderson, J.B., and Fillon, R.H., eds., Late Quaternary Stratigraphic Evolution of the Northern Gulf of Mexico Margin: SEPM, Special Publication 79, p. 1-23.

Back, S., Hocker, C., Brundiers, M., B., and Kukla, P. A., 2006, Three dimensional-seismic coherency signature of Niger Delta growth faults: integrating sedimentology and tectonics: Basin Research, v. 18, p. 323-337.

Baudon, C. and Cartwright, J., 2008, Early stage evolution of growth faults: 3D seismic insights from the Levant Basin, Eastern Mediterranean: Journal of Structural Geology, v. 30, p. 888-898.

Berryhill, H.L.J., 1987, Late Quaternary facies and structure, northern Gulf of Mexico: American Association of Petroleum Geologists Studies in Geology, v. 23, p. 289.

Bhattacharya, J.P. and R.K. Davies, 2001, Growth faults at the prodelta to delta-front transition, Cretaceous Ferron sandstone, Utah: Marine and Petroleum Geology, v. 18, p. 525 – 534.

Bhattacharya, J.P. and Davies, R.K., 2004, Sedimentology and structure of growth faults at the base of the Ferron Sandstone Member along Muddy Creek, Utah, *in* Chidsey, T.C., Adams, R.D., and Morris, T.H., eds., The Fluvial-Deltaic Ferron Sandstone: Regional-to-wellbore-scale outcrop analog studies and applications to reservoir modeling: AAPG, Studies in Geology 50, p. 279-304.

Bischke, R. E., 1994, Interpreting sedimentary growth structures from well log and seismic data (with examples): AAPG Bulletin, v. 78, p.873-892.

Brown, L.F., Jr., Cleaves, A.W., II, and Erxleben, A.W., 1973, Pennsylvanian depositional sstems in North-Central Texas—a guide for interpreting terrigenous clastic facies in a cratonic basi: Bureau of Economic Geology Guidebook No. 14, University of Texas at Austin, p. 122.

Brown, L.F., Jr., Loucks, R.G., Trevion, R.H., and Hammes, U., 2004, Understanding growth-faulted intra-slope basins by applying sequence stratigraphic principles: examples from the south Texas Oligocene Frio Formation: AAPG Bulletin, v. 88, p. 1501-1522.

Cartwright, J., Bouroullec, R., James, D., and Johnson, H., 1998, Polycyclic motion of some Gulf Coast growth faults from high-resolution displacement analysis: Geology, v. 26, no. 9, p. 819-822.

Castelltort, S., Pochat, S., and Van Den Driessche, J., 2004, Using T-Z plots as a graphical method to infer lithological variations from growth strata: Journal of Structural Geology, v. 26, p. 1425-1432.

Diegel, F. A., J. F. Karlo, D. C. Schuster, R. C. Shoup, and P. R. Tauvers, 1995, Cenozoic structural evolution and tectono-stratigraphic framework of the northern Gulf Coast continental margin, *in* M. P. A. Jackson, D. G. Roberts, and S. Snelson, eds., Salt tectonics: a global perspective: AAPG Memoir 65, p. 109–151.

Edwards, M. B., 1976, Growth faults in upper Triassic deltaic sediments, Svalbard: AAPG Bulletin, v. 60, p. 341–355.

Edwards, M.B., 1995, Differential subsidence and preservation potential of shallow-water Tertiary sequences, northern Gulf Coast Basin, USA, *in* Plint, A.,, G., ed., Sedimentary facies analysis: International Association of Sedimentologists Special Publication 22, p. 497-509.

Evamy, B.D., Haremboure, J., Kamerling, P., Knapp, W.A., Moloy, F.A., and Rowlands, P.H., 1978, Hydrocarbon habit of Tertiary Niger Delta: American Association of Petroleum Geologist Bulletin, v. 62, p. 1-39.

Galloway, W.E., Hobday, D.K., and Magara, K., 1982, Frio Formation of Texas Gulf Coastal Plain-depositional systems, structural framework and hydrocarbon distribution: AAPG Bulletin, v. 66, p. 649-688.

Galloway, W.E., Ganey-Curry, P.E., Li, X., and Buffler, R.T., 2000, Cenozoic depositional history of the Gulf of Mexico basin: AAPG Bulletin, v. 84, no. 11, p. 1743-1774.

Liner, C, 2004, Elements of 3D Seismology: PenWell Corporation, Tusla, Oklahoma, ed. M. Patterson, p.454-456.

McCulloh, R. P., 1988, Differential fault-related early Miocene sedimentation, Bayou Herbert area, southwestern Louisiana: AAPG Bulletin, v. 72, p. 249-263.

Mansfield, C.S., and Cartwright, J.A., 1996, High resolution displacement mapping from 3-D seismic data: Journal of Structural Geology, v. 24, p. 847-859.

Nemec, W., Steel, R.L., Gjelberg, J., Collinson, J.D., Prestolm, E., and Oxevad, I.E., 1998, Anatomy of a collapsed and re-established delta front in Lower Cretaceous of Eastern Spritsburg-gravitational sliding and sedimentation processes: AAPG Bulletin, v. 74, p. 454-476.

Owoyemi, A.O., and Willis, B.J., 2006, Depositional patterns across syndepositional normal faults, Niger Delta, Nigeria: Journal of Sedimentary Research, v. 76, p.346-363.

Peel, F.J., C.J. Travis, and J.R. Hossack, 1995, Genetic structural provinces and salt tectonics of the Cenozoic offshore U.S. Gulf of Mexico: a preliminary analysis, *in* M.P.A. Jackson, D.G. Roberts, and S. Snelson, eds., Salt tectonics: a global perspective: AAPG Memoir 65, p.153 – 175.

Pochat, S., Castelltort, S., Van Den Driessche, J., Besnart, K., and Gumiaux, C., 2004, A simple method of determining sand/shale ratios from seismic analysis of growth faults: An example from upper Oligocene to lower Miocene Niger Delta deposits: AAPG Bulletin, v. 88, no. 10, p. 1357-1367.

Roberts, H.H., Fillon, R.H., Kohl, B., Robalin, J.M., and Sydow, J.C., 2004, Depositional architecture of the Lagniappe delta: sediment characteristics, timing of depositional events, and temporal relationship with adjacent shelf-edge deltas, *in* Anderson, J.B., and Fillon, R.H., eds., Late Quaternary Stratigraphic Evolution of the Northern Gulf of Mexico Margin: SEPM, Special Publication 79, p. 143-188.

Rider, M.H., 1978, Growth faults in the Carboniferous of Western Island: AAPG Bulletin, v. 62, p. 2191-2213.

Salvador, A., 1987, Late Triassic-Jurassic paleogeography and origin of Gulf of Mexico basin: AAPG Bulletin, v. 71, no. 4, p. 419-451.

Sydow, J., and Roberts, H.H., 1994, Stratigraphic framework of a late Pleistocene shelf-edge delta, northeast Gulf of Mexico: AAPG Bulletin, v. 78, p. 1276–1312.

Tearpock, D., and Bishke, R.E., 1991, Applied subsurface geological mapping: New York, Prentice Hall, p. 648.

Thorsen, C.E., 1963, Age of growth faulting in southeast Louisiana: Gulf Coast Association of Geological Societies Transactions, v. 13, p. 103-110.

Wadsworth, A., H., 1953, Percentage of thinning chart: A new technique in subsurface geology: AAPG Bulletin, v. 37, p. 158-162.

Wellner, J.S., Sarzalejo, S., Lagoe, M., and Anderson, J.B., 2004, Late Quaternary stratigraphic evolution of the West Louisiana/East Texas continental shelf, *in* Anderson, J.B., and Fillon, R.H., eds., Late Quaternary Stratigraphic Evolution of the Northern Gulf of Mexico Margin: SEPM, Special Publication 79, p. 217-235.

Wignall, P.B., and Best, J.L., 2004, Sedimentology and kinematics of a large, retrogressive growth-fault system in Upper Carboniferous deltaic sediments, western Ireland: Sedimentology, v. 52, p. 1343-1358.

Winker, C. D., and M. B. Edwards, 1983, Unstable progradational clastic shelf margins, *in* D. J. Stanley and G. T. Moore, eds., The shelf-break — critical interface on continental margins: SEPM Special Publication 33, 139–157.

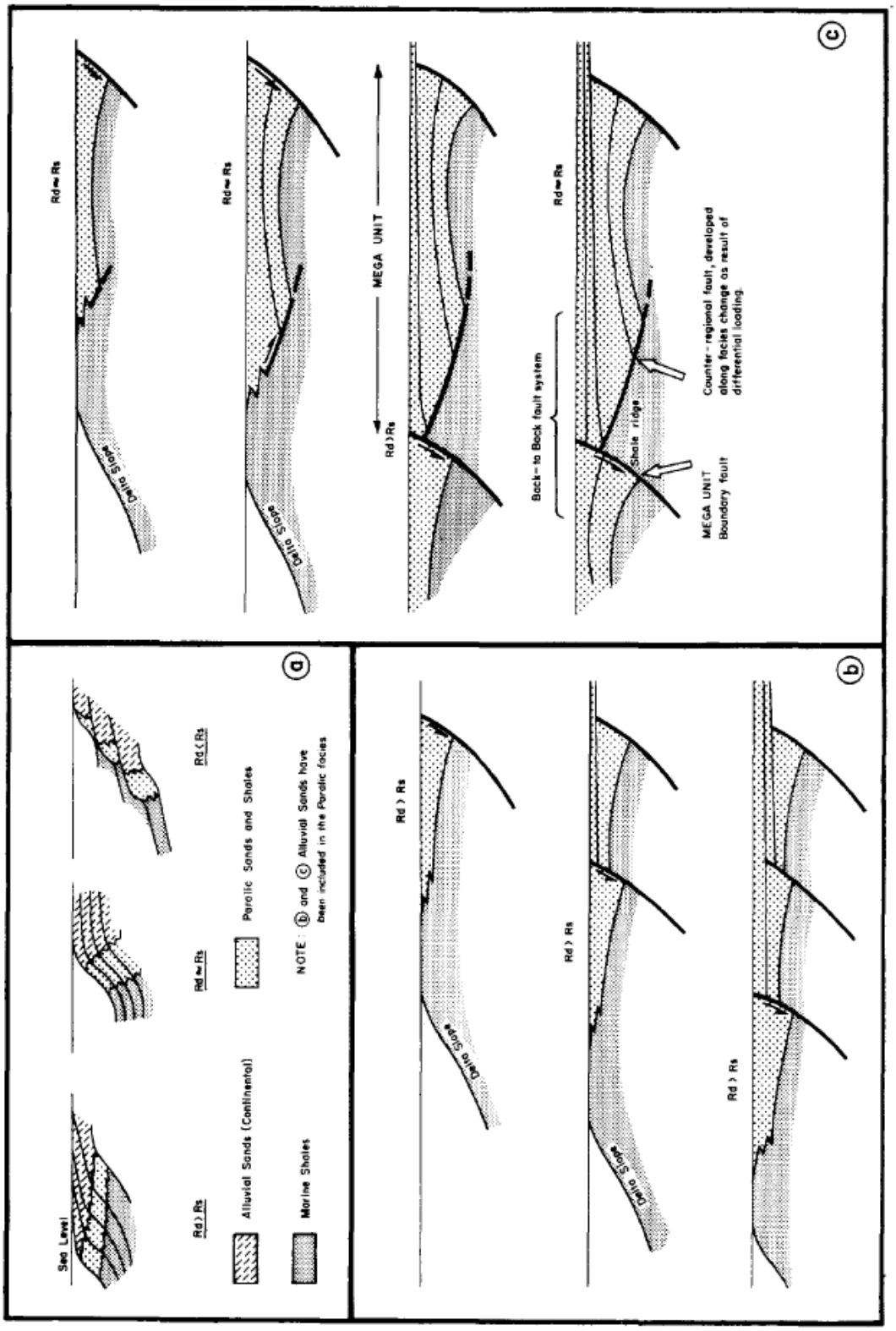

Figure 1: A) Schematic development of growth faults of the Tertiary Niger Delta. Rd=rate of deposition, Rs=rate of subsidence. B) shows the development of growth faults when Rd> Rs, C) shows the development of growth faults when Rs=Rd (From Evamy *et al.,* 1978).

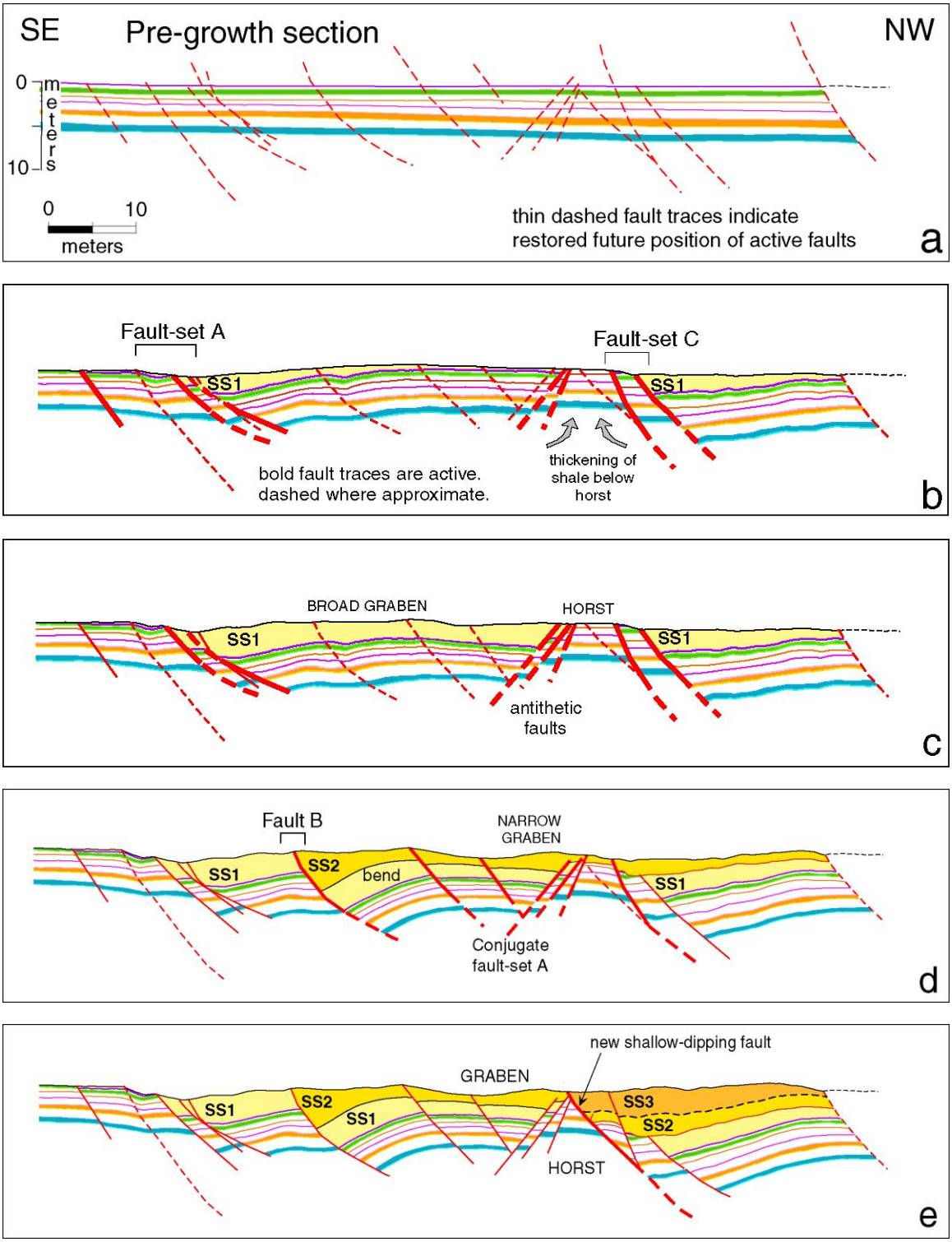
SE
Pre-growth section
NW
0
meters
10
0
10
meters
thin dashed fault traces indicate
restored future position of active faults
a
Fault-set A
Fault-set C
SS1
SS1
bold fault traces are active.
dashed where approximate.
thickening of
shale below
horst
b
BROAD GRABEN
HORST
SS1
SS1
antithetic
faults
c
Fault B
NARROW
GRABEN
SS1
SS2
bend
SS1
Conjugate
fault-set A
d
new shallow-dipping fault
GRABEN
SS1
SS2
SS1
SS3
SS2
HORST
e

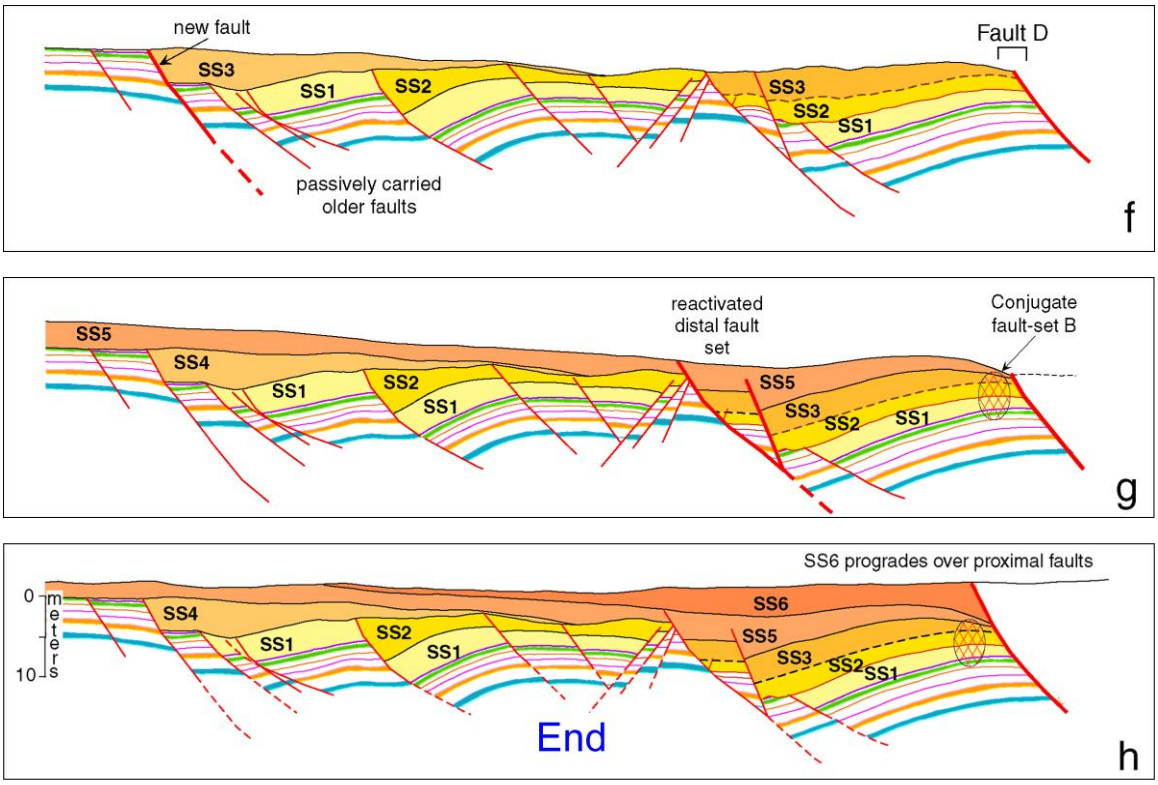

Figure 2: Kinematic restoration of Muddy Creek growth faults in the Ferron Sandstone, Utah. Fault initiation shows no systematic landward or basinward pattern (From Bhattacharya and Davies, 2001, 2004).

A)

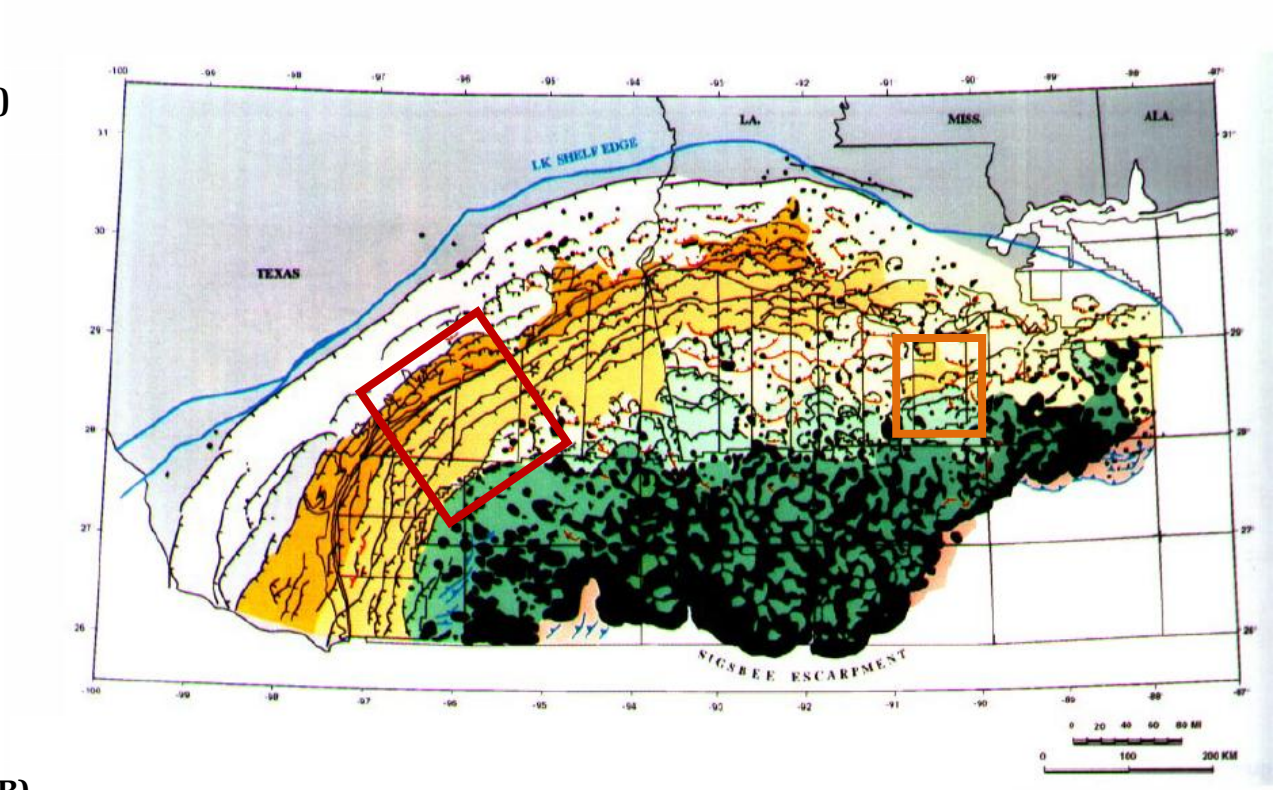

B)

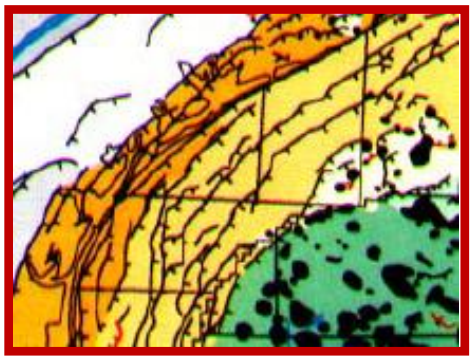

Figure 3: Structural summary map of the northern Gulf of Mexico Basin A) showing large arcuate growth faults dipping basinward, in black. Counter-regional faults in red. The tectono-stratigraphic provinces of the Northern Gulf of Mexico. My study area lies in the Plio-Pleistocene detachement province to the south (light green) and the salt-dome minibasin province to the north (yellow) in the orange box; B) Zoomed in version of red box, showing large-scale growth faults that have relay ramps and branching (From Diegal *et al.*, 1995).

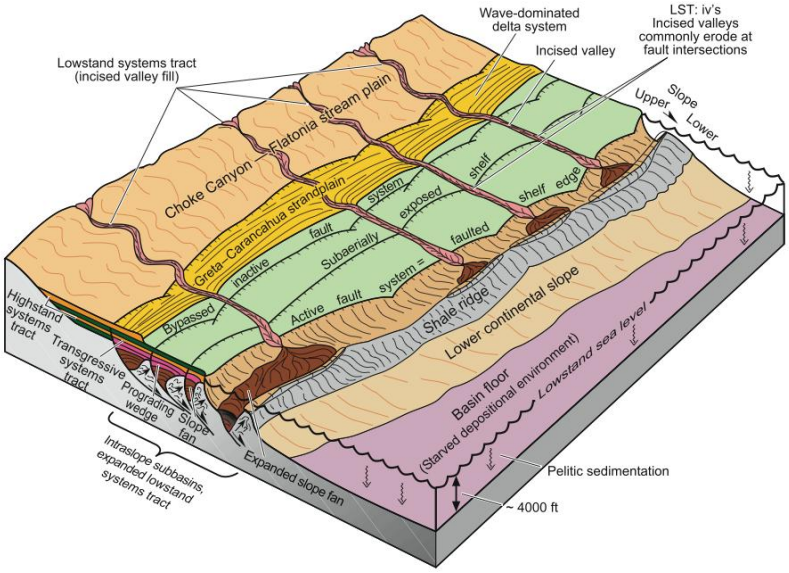

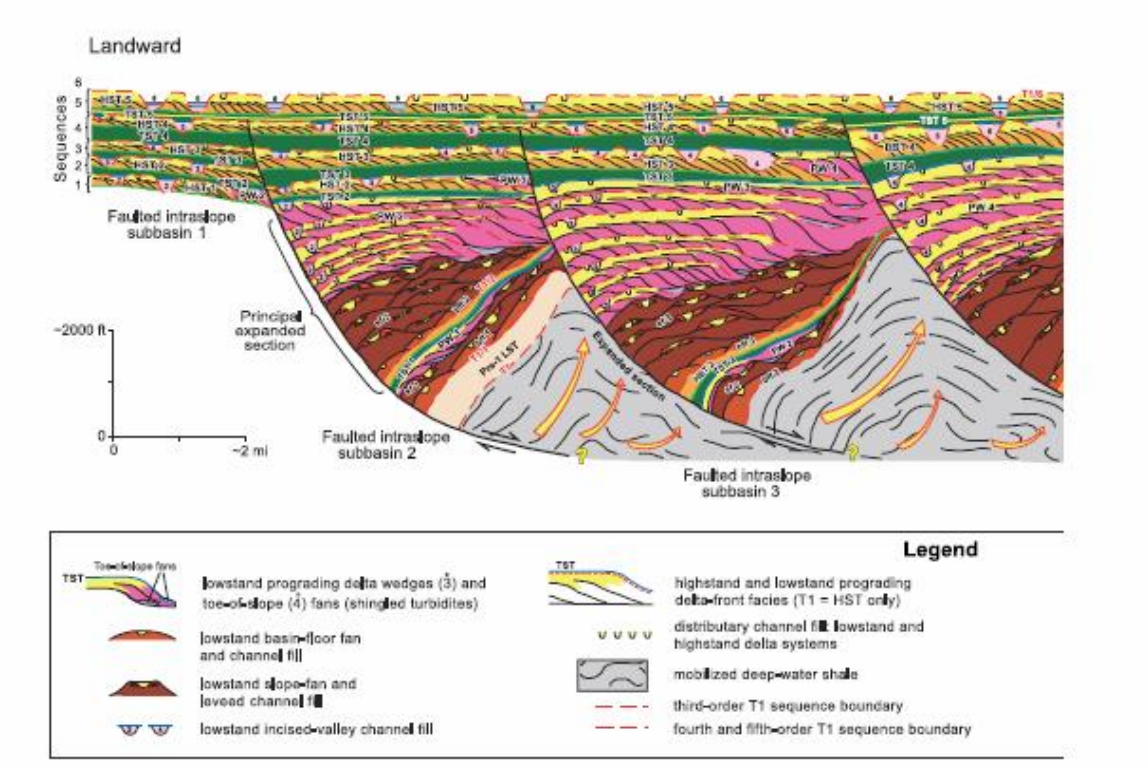

Figure 4: Interpretation of Gulf of Mexico growth faults in cross section from high-resolution 3D seismic data. See the basinward fault initiation and accommodation created at shelf edge from the over-steepened shales (From Brown *et al.*, 2004).

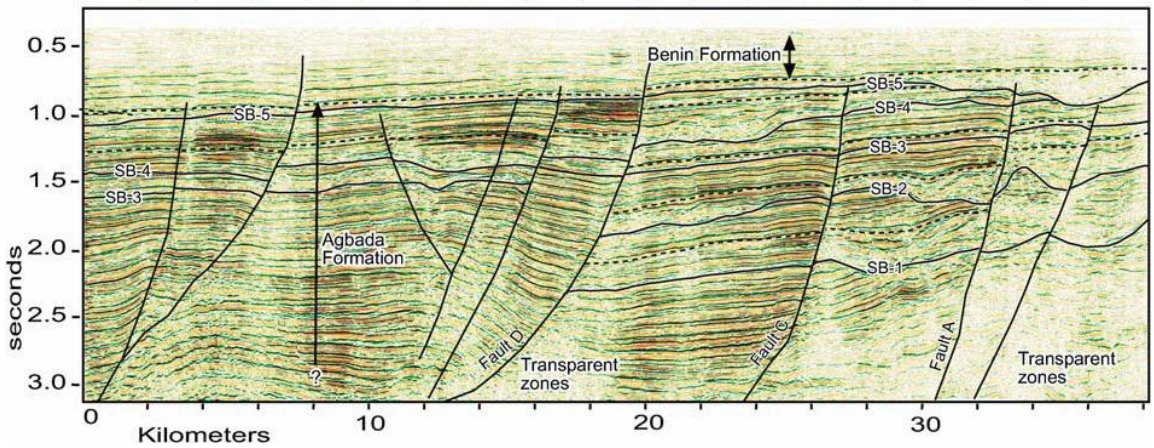

Figure 5: Seismic line of region scale growth faults from the Niger Delta that shows fault locations (From Owoyemi and Willis, 2004).

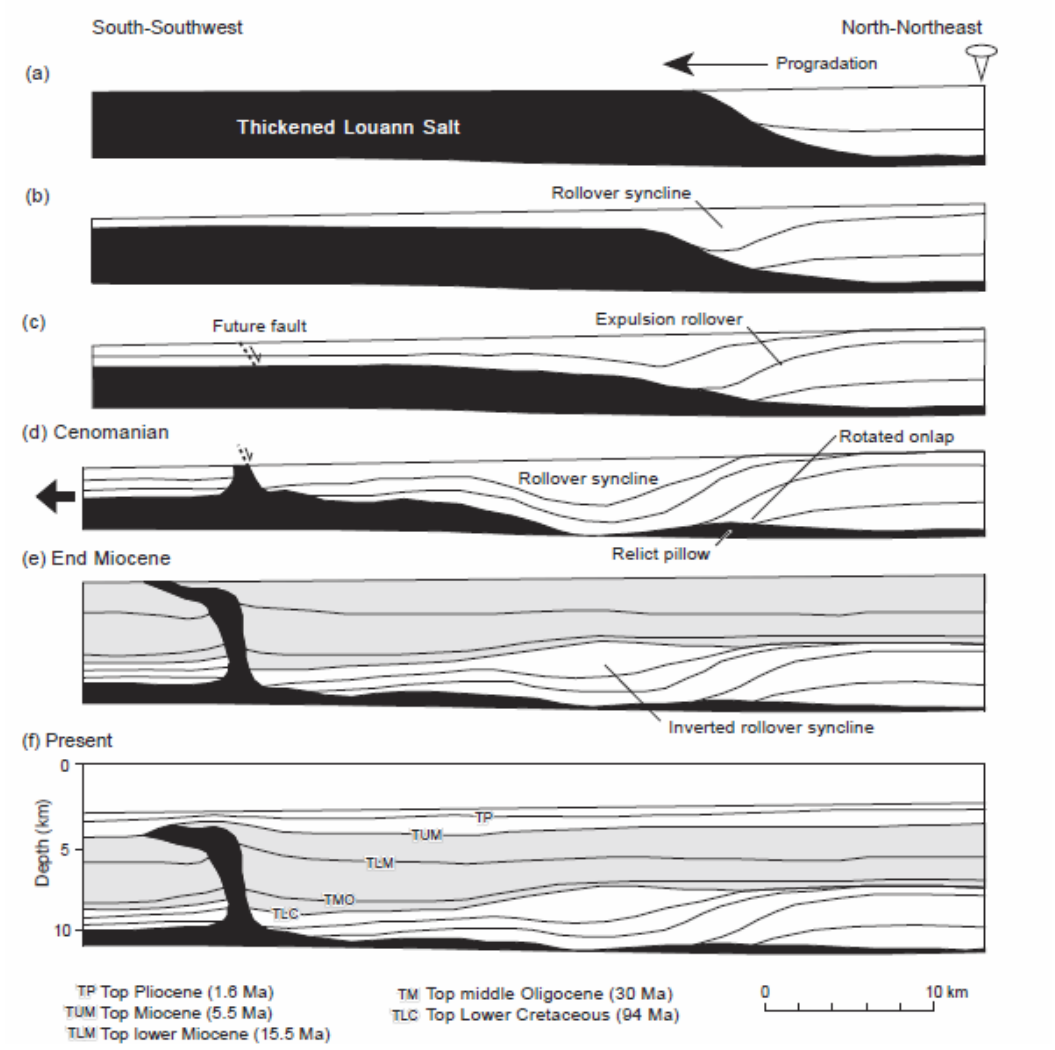

Figure 6: Salt diapirism created additional accommodation in the form of minibasins that were able to collect and contain sediment from later prograding deltas (From Ge *et al.,* 1997).

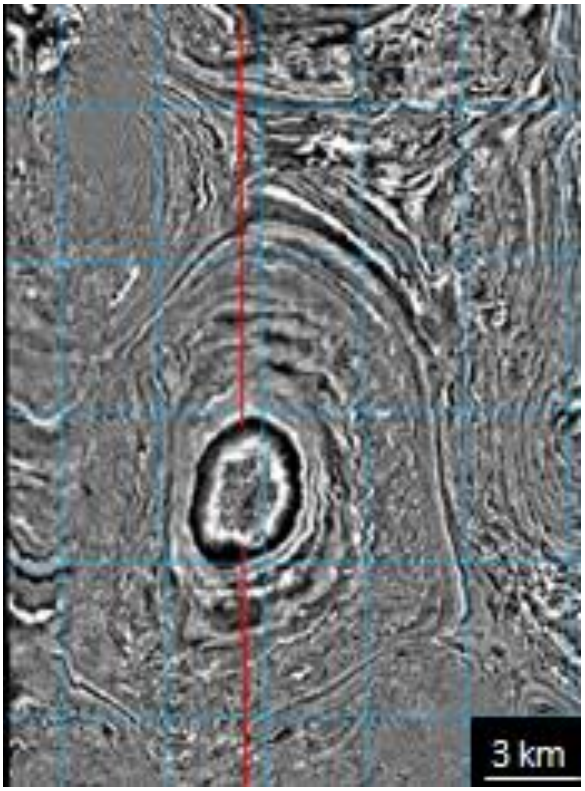

Figure 7: Time slice of the minibasin at 1.5 seconds. Note the minibasin in the center that is flanked by residual vertical salt bodies to the northwest and the southeast. The red line marks the location of the seismic line in Fig. 11a and 11b.

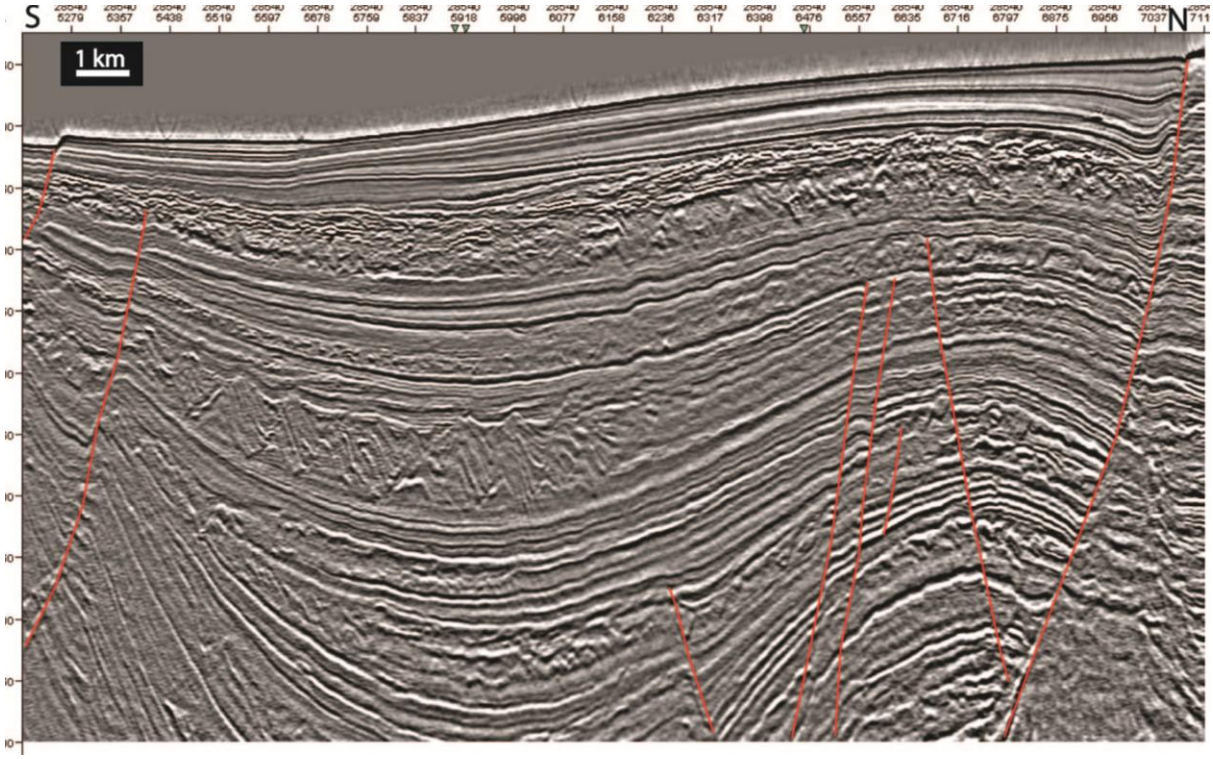

Figure 8a: 2D Interpretation window of dip view of minibasin. Progradation of delta basinward, towards the south. Salt diapirs flank the minibasin to the North and South. TWT in ms. Large faults are marked in red. Water depths range from 190 m to 415 m.

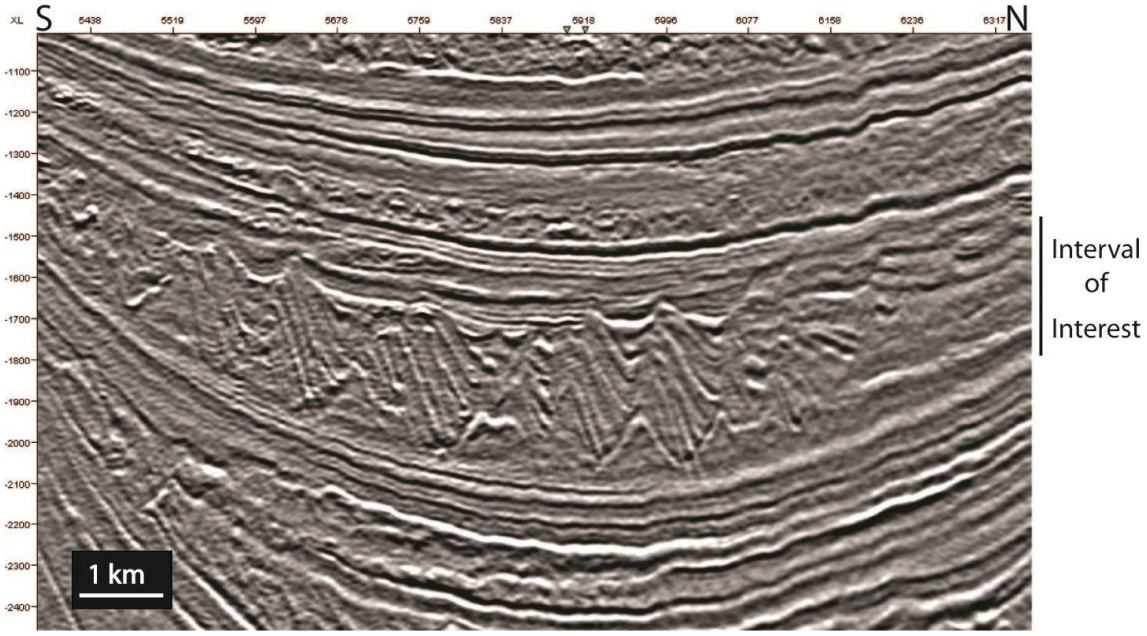

Figure 8b: Intra-deltaic deformation fully confined within one sequence. Note listric, normal faulting dipping basinward, toward the South. Interval of interest is 560 m thick. TWT in ms.

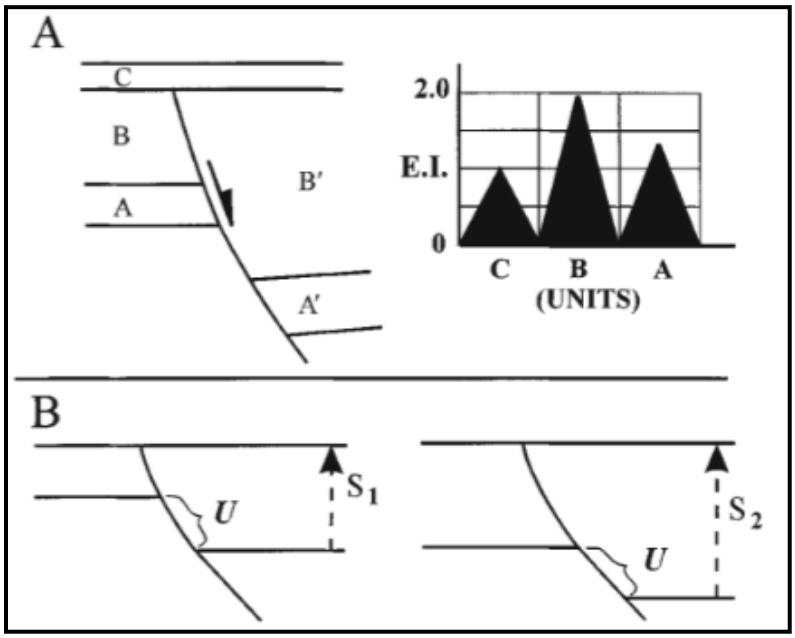

Figure 9: Expansion index (E.I.) depicting behavior of growth fault. A) Growth fault showing activity in units A and B expressed in E.E. values >1.0, in which E.I. equals the ratio of the stratigraphic thickness in hanging wall to footwall. Activity of fault ends with unit C, giving it an E.I. of 1.0. B) Shows sections of two growth faults with different values of E.I., but same slip rates resulting from different sedimentation rates S1>S2 (From Cartwright *et al*., 1998).

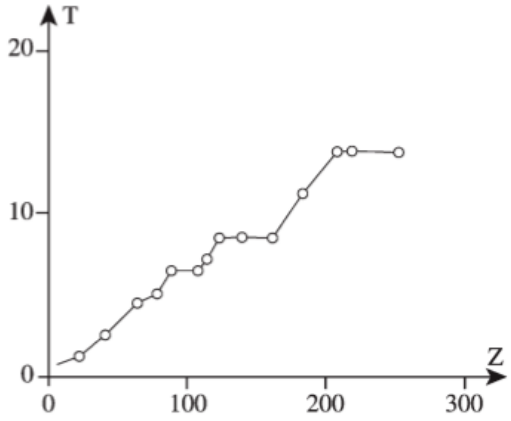

Figure 10: Example of throw (T vertical axis) versus depth (Z, horizontal axis) plot constructed from high-resolution seismic across a growth fault in the Gulf Coast, offshore Texas, late Pleistocene to recent (modified from Cartwright *et al.,* 1998). Values in meters. The positive slope represents phases of growth and horizontal segments represent phases of fault inactivity (From Castelltort *et al.,* 2004).

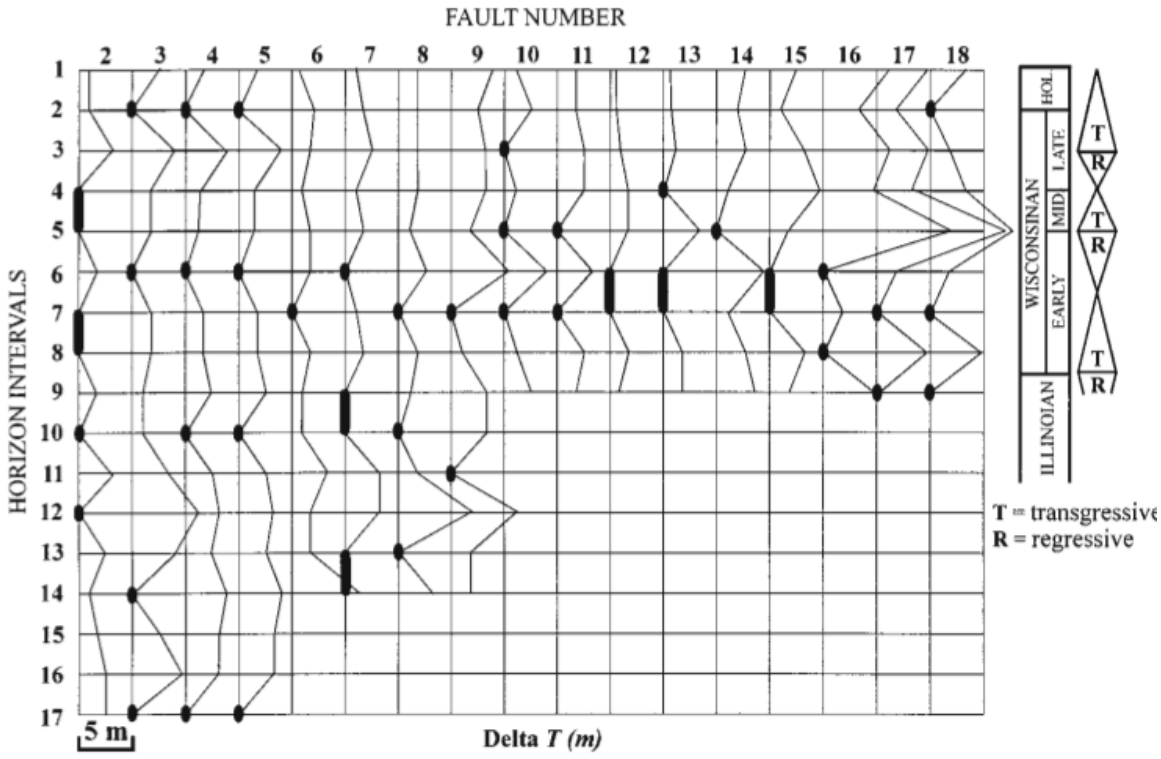

Figure 11: Plot of throw versus horizon interval for 17 faults from study transect. Periods of inactivity are the heavy lines. Plotted alongside is a chronostratigrphic correlation from Berryhill (1987), with transgressive-regressive cyclostratigraphy. Spacing between horizons is not indicative of a specific time interval (From Cartwright *et al.,* 1998).

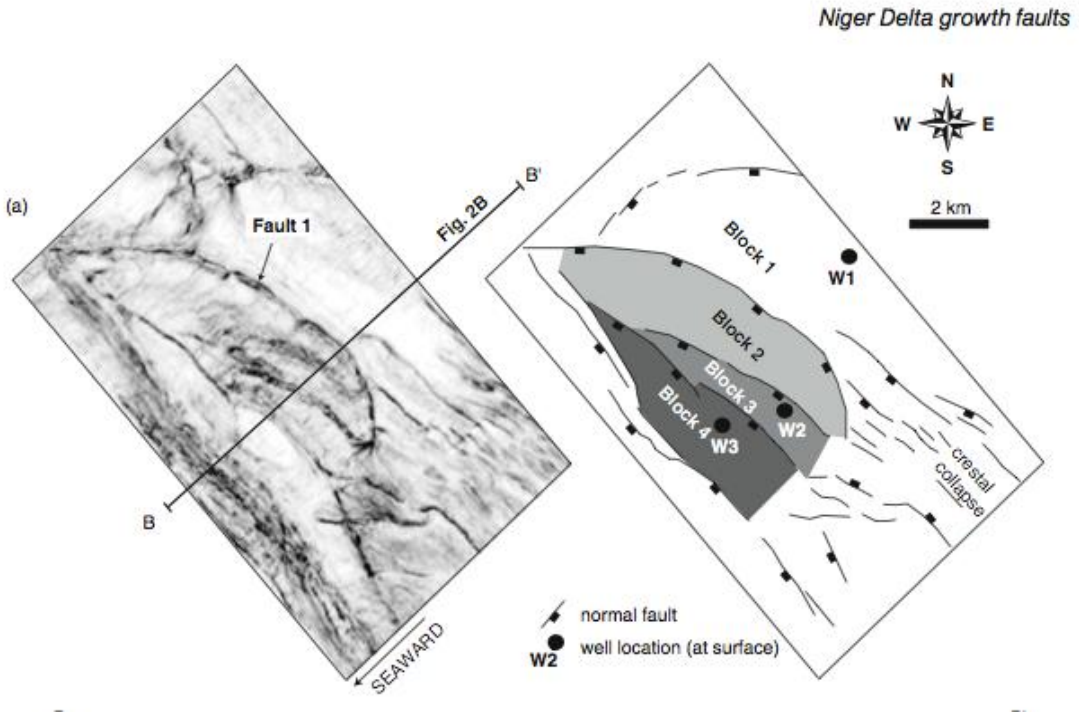

Figure 12: Seismic coherency horizon slice at 1.5s (TWT) and interpretation. High coherency values are in white and low coherency values are in black (From Back *et al.,* 2006).

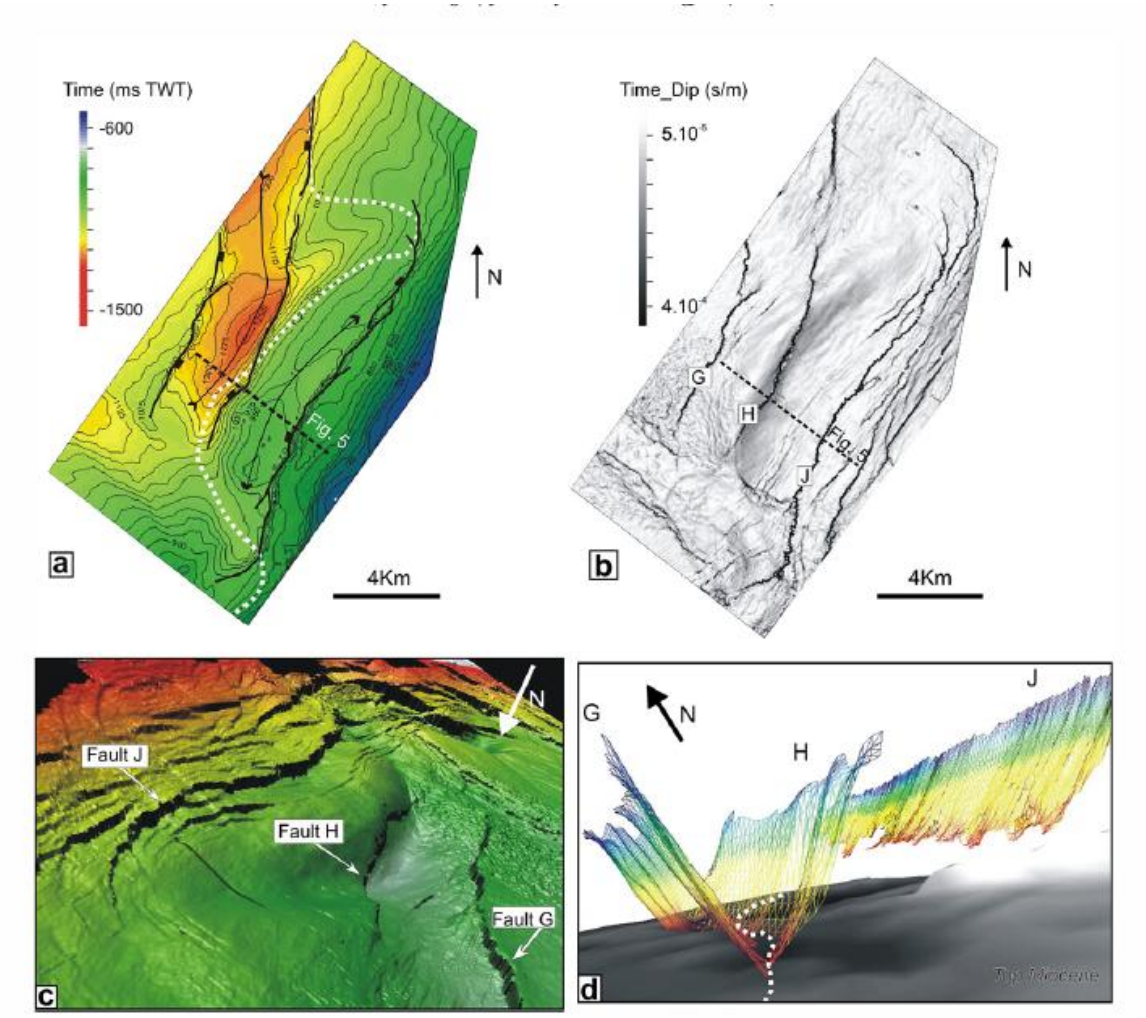

Figure 13: A) TWT contour map of study area spaced at 25 ms with high values in red and low values in red. B) Dip map that shows the traces of the main faults. C) Geoviz image of Pleistocene horizon (Fault gap map). D) Geoviz visualization of geometry of faults (From Baudon and Cartwright, 2008).

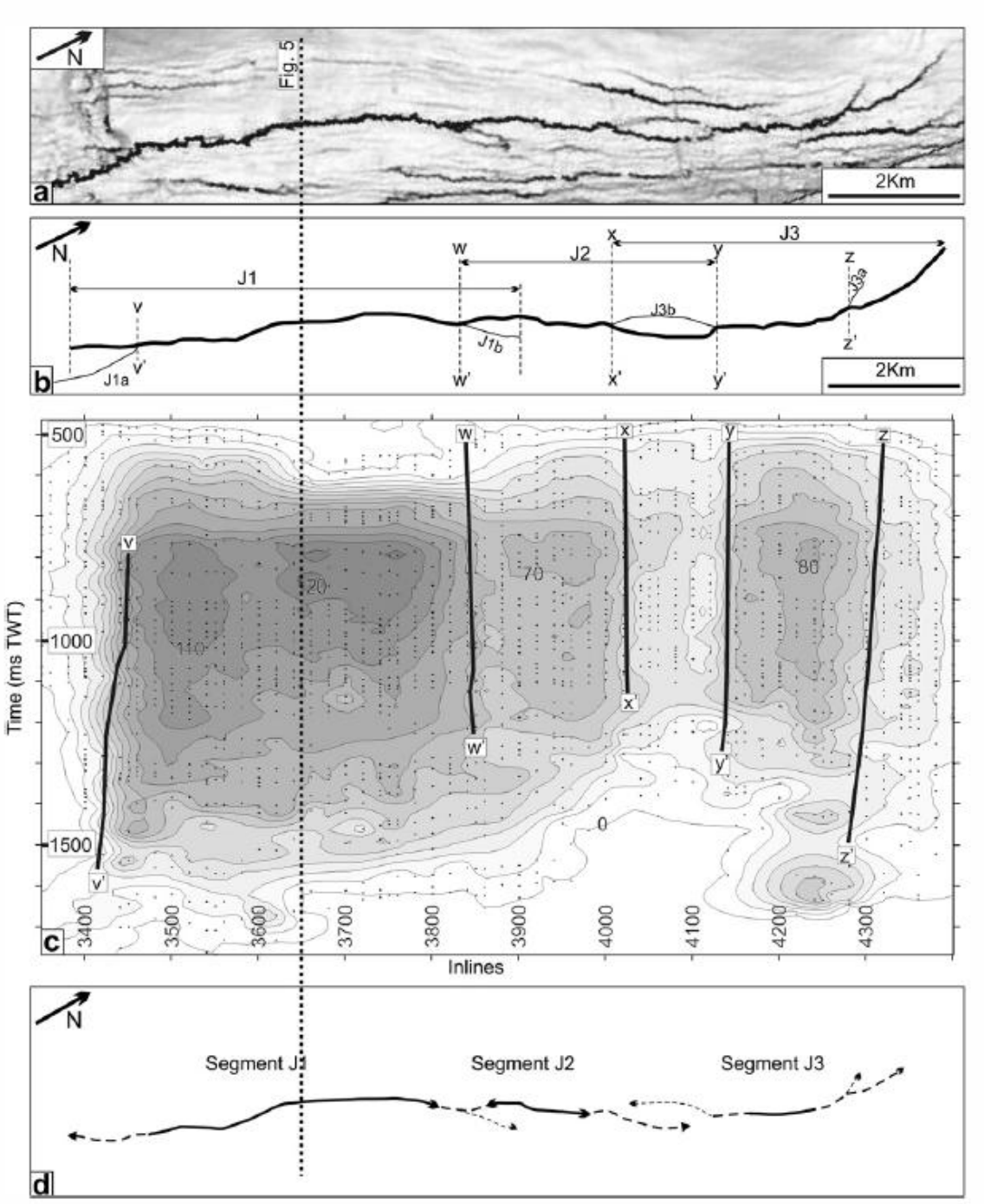

Figure 14: A) Dip map of Pleistocene horizon of Fault. B) Schematic representation of fault trace and segments. C) Throw contour plot for fault J spaced every 10 ms TWT. D) Schematic showing lateral segment that formed Fault J (From Baudon and Cartwright, 2008).

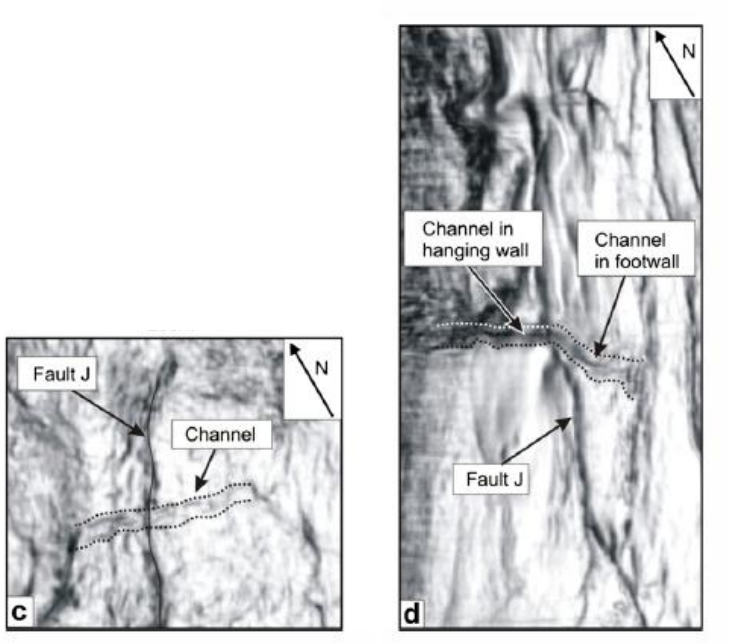

Figure 15: Coherency slices of mapped river channels depicting channel diversion due to faulting. C) Coherency slice at 1416 ms TWT showing a channel cross-cut by fault J, within same prekinematic sequence. D) Coherency slice at 528 ms TWT showing the change of direction of a channel being cross-cut by fault J (From Baudon and Cartwright, 2008).

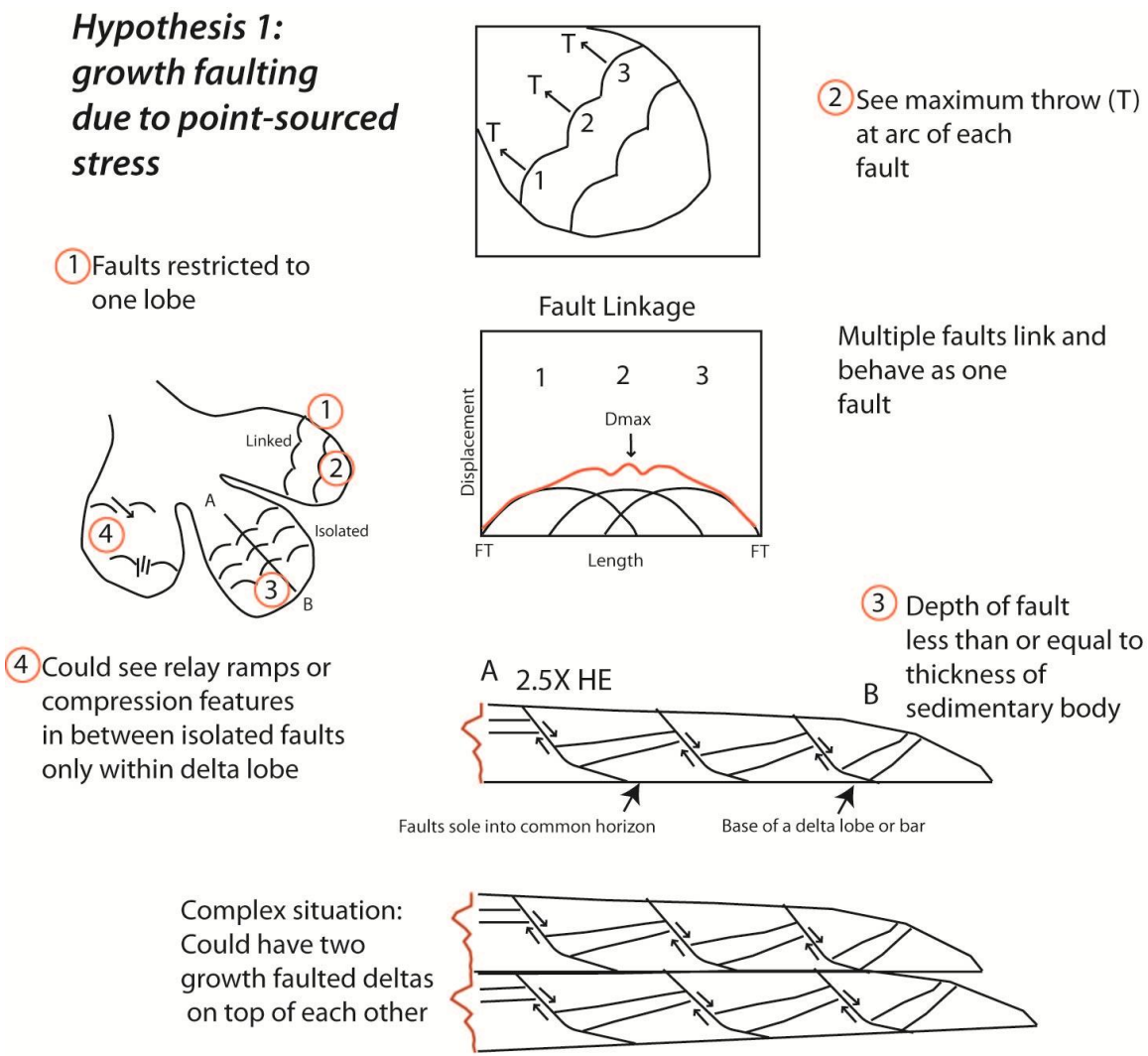

Figure 16: Hypothesis 1 shows predicted fault geometries and linkage of growth faults due to distributive stress. Depicts predicted plan view of faults, predicted fault linkage patterns, predicted cross-sectional view of faults

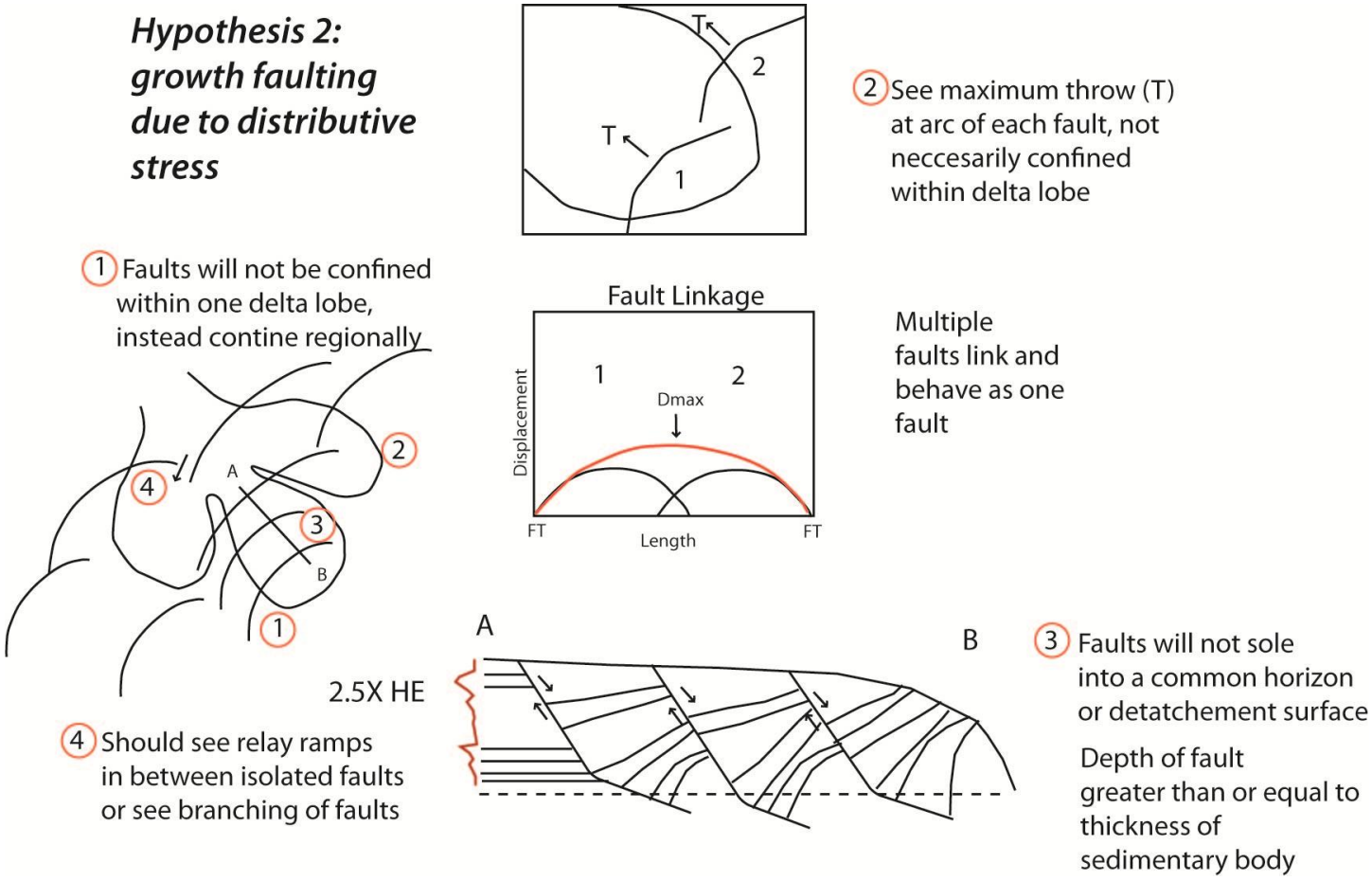

Figure 17: Hypothesis 2 shows predicted fault geometries and linkage of growth faults due to distributive stress. Depicts predicted plan view of faults, predicted fault linkage patterns, predicted cross-sectional view of faults

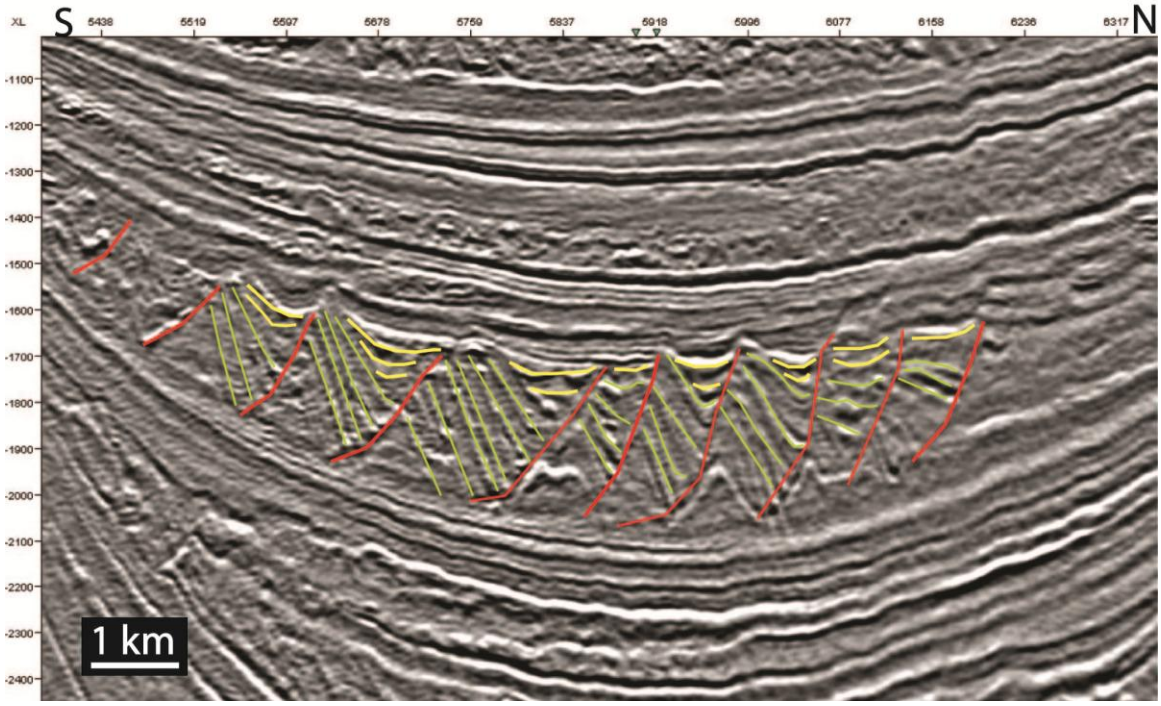

Figure 18a: 2D seismic interpretation window with growth faults mapped in red, continuous reflections within rotated blocks in green, and inflilling sediment in yellow. TWT in ms.

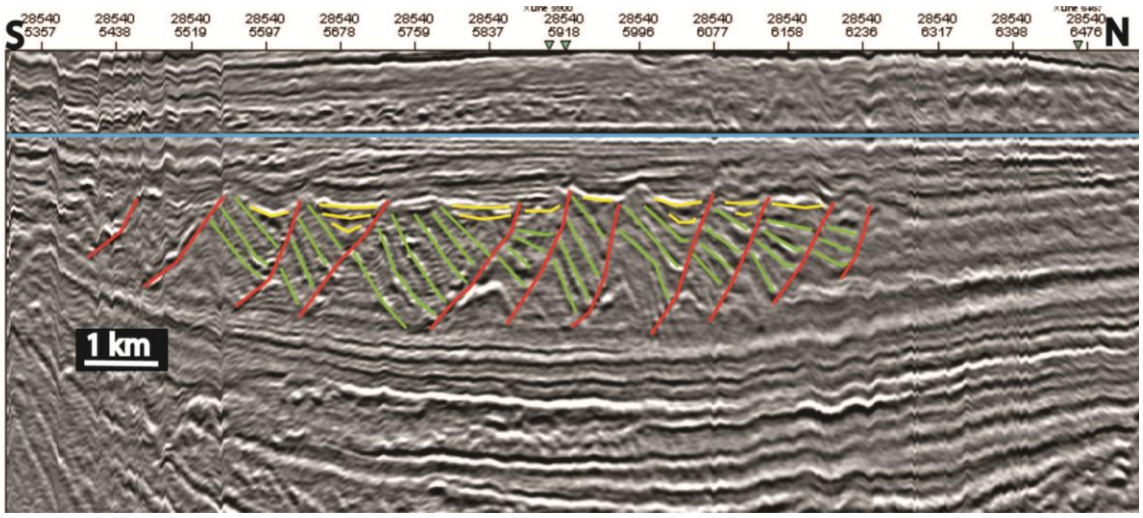

Figure 18b: 2D seismic interpretation window on flattened horizon with growth faults mapped in red, continuous reflections within rotated blocks in green, and inflilling sediment in yellow. TWT in ms.